nature genetics

Targets and dynamics of promoter DNA methylation during early mouse development

Julie Borgel[1], Sylvain Guibert[1], Yufeng Li[2], Hatsune Chiba[2], Dirk Schübeler[3], Hiroyuki Sasaki[2], Thierry Forné[1] & Michael Weber[1]

DNA methylation is extensively reprogrammed during the early phases of mammalian development, yet genomic targets of this process are largely unknown. We optimized methylated DNA immunoprecipitation for low numbers of cells and profiled DNA methylation during early development of the mouse embryonic lineage *in vivo*. We observed a major epigenetic switch during implantation at the transition from the blastocyst to the postimplantation epiblast. During this period, DNA methylation is primarily targeted to repress the germline expression program. DNA methylation in the epiblast is also targeted to promoters of lineage-specific genes such as hematopoietic genes, which are subsequently demethylated during terminal differentiation. *De novo* methylation during early embryogenesis is catalyzed by Dnmt3b, and absence of DNA methylation leads to ectopic gene activation in the embryo. Finally, we identify nonimprinted genes that inherit promoter DNA methylation from parental gametes, suggesting that escape of post-fertilization DNA methylation reprogramming is prevalent in the mouse genome.

Mammalian development is regulated by sequence-specific transcription factors, but it also entails epigenetic modifications that establish heritable cellular memories[1]. DNA methylation occurs on cytosines, mostly in the context of CpG dinucleotides, and is essential for embryonic development[2,3]. DNA methylation is extensively reprogrammed during early development, with the paternal genome being demethylated shortly after fertilization, whereas the maternal genome is progressively demethylated by lack of maintenance methylation[4–6]. In mouse, *de novo* methylation is initiated around implantation mostly in embryonic cells, whereas extraembryonic cells have lower levels of DNA methylation, as visualized by immunostaining[7]. However, sequences undergoing dynamic DNA methylation during early embryogenesis remain unknown.

Cytosine methylation is rare at regulatory regions containing CpG islands; however, a small fraction of CpG islands is methylated in somatic cells[8–10]. Pluripotency genes are preferential targets for promoter DNA methylation[11–13], indicating that DNA methylation is linked to the control of pluripotency. This is supported by the observations that demethylation of pluripotency genes is required to reprogram somatic cells to a pluripotent state and that interfering with DNA methylation improves the rate of reprogramming[14,15]. DNA methylation may also participate in maintaining cellular identity by targeting developmental genes such as *Pax6*, *Hox* family genes or germline genes[8,9,16]. However, most mapping studies have been performed in cultured cellular models that do not necessarily recapitulate the situation *in vivo*[12,17], illustrating the need to identify targets of DNA methylation *in vivo*.

Epigenetic marks can be inherited through cell division but potentially also through generations. Inheritance of epigenetic information has been implicated in non-Mendelian transmission of phenotypes such as the coat color controlled by the *Agouti viable yellow* allele or defects linked to environmental factors[18]. The only examples of sequences that resist demethylation after fertilization are germline differentially methylated regions (DMRs) in imprinted loci. It has also been shown that intracisternal A-particles (IAPs) partially resist demethylation in preimplantation embryos[19]. Alternative mechanisms for epigenetic inheritance could involve RNAs or modified histones that transmit information from gametes to early embryos[20,21].

Several techniques have emerged to map DNA methylation genome wide. Methods combining bisulfite treatment with deep sequencing provide information at single-nucleotide resolution, yet they require enormous sequencing efforts to give information at individual sequences[22,23]. Immunocapturing approaches such as methylated DNA immunoprecipitation (MeDIP) constitute good alternatives at reasonable costs[24]. However, available protocols require large amounts of DNA that preclude studies on limited cellular populations. Here we report an optimized MeDIP for a small amount of cells and use it to profile DNA methylation during early development of the mouse embryonic lineage. We show that DNA methylation is targeted to specific gene promoters during implantation and that this methylation is required to maintain gene repression. In addition, we describe for the first time post-fertilization inheritance of gametic DNA methylation at nonimprinted genes.

[1]Institute of Molecular Genetics, Centre National de la Recherche Scientifique (CNRS) UMR 5535, Université Montpellier 2, Université Montpellier 1, Montpellier, France. [2]Department of Molecular Genetics, Medical Institute of Bioregulation, Kyushu University, Higashi-ku, Fukuoka, Japan. [3]Friedrich Miescher Institute for Biomedical Research, Basel, Switzerland. Correspondence should be addressed to M.W. (michael.weber@igmm.cnrs.fr).

Received 8 April; accepted 14 September; published online 7 November 2010; doi:10.1038/ng.708

RESULTS

An optimized MeDIP protocol for low amounts of DNA

To map DNA methylation in early mouse embryos, we optimized the MeDIP-on-ChiP procedure to immunoprecipitate methylated DNA from 150 ng of DNA (Online Methods). We subsequently amplified input and MeDIP fractions by whole-genome amplification (WGA). To validate this procedure, we show by quantitative PCR (qPCR) that enrichments with MeDIP-WGA on 150 ng of DNA and with standard MeDIP on 2 μg of DNA are similar (**Supplementary Fig. 1a**). To assess the accuracy of our optimized protocol genome wide, we hybridized MeDIP-WGA samples from 150 ng of DNA from embryos at embryonic day (E) 9.5, as well as from 20 pooled unamplified MeDIPs, each prepared from 2 μg of the same DNA, on NimbleGen arrays covering all gene promoters. The resulting profiles indicated that oligonucleotide log2 ratios are very similar with both MeDIP-WGA and pooled MeDIPs (**Supplementary Fig. 1b**). We only observed discrete genomic regions that showed inaccurate profiles with MeDIP-WGA as compared to pooled MeDIPs (**Supplementary Fig. 1c**). To correlate the profiles, we averaged oligonucleotide log2 ratios in the region −400 bp to +400 bp from all transcription start sites. A comparison on chromosome 14 showed that most gene promoters enriched with pooled MeDIPs are also enriched with MeDIP-WGA (**Supplementary Fig. 1d**). When comparing all genes, we observed a good correlation between average log2 ratios measured with pooled MeDIPs and with MeDIP-WGA on 150 ng of DNA ($r = 0.81$; **Fig. 1a**). This shows that our optimized MeDIP protocol allows accurate profiling of DNA methylation from low amounts of cells.

DNA methylation in the developing embryonic lineage

We hybridized MeDIP samples from E3.5 blastocysts, epiblasts from E6.5 embryos and E9.5 embryos to NimbleGen HD2 arrays covering 11 kb of gene promoters, which represents 10% coverage of the mouse genome (**Fig. 1b**). In E3.5 blastocysts, because the genome is globally hypomethylated, MeDIP ratios mostly reflect random background and are equally distributed along tiled regions, although we noted a slight increase of the ratio in gene bodies (**Fig. 1c** and **Supplementary Fig. 2a**). Consistent with global hypomethylation, E3.5 blastocysts showed no correlation between MeDIP signals and CpG content at the promoters (**Supplementary Fig. 2b**) and a very low fraction of enriched promoters (**Supplementary Fig. 2c**). In E6.5 epiblasts and E9.5 embryos, DNA methylation was low around transcription start sites (TSS) and was higher in gene bodies as compared to intergenic regions (**Fig. 1c**)[22,25,26]. When classifying promoters as low (LCPs), intermediate (ICPs, weak CpG islands) or high CpG promoters (HCPs, strong CpG islands; Online Methods), we observed that hypomethylation around the TSS is a hallmark of HCPs but not of LCPs or ICPs (**Supplementary Fig. 2a**). Consistently, a large fraction of LCPs and ICPs are hypermethylated in E6.5 epiblasts and E9.5 embryos, whereas HCPs remain mostly hypomethylated (**Supplementary Fig. 2b**,**c**), which recapitulates previous results in mammalian cells[9,12,13].

Importantly, we detected high MeDIP enrichments in E3.5 blastocysts at several imprinted genes carrying germline DMRs (*Plagl1*, *Snrpn*, *Peg1*, *Peg3*, *Peg10* and *Nnat*) but not in those carrying secondary DMRs that are established postimplantation (**Fig. 1d** and **Supplementary Fig. 3**), which validates our approach. We also detected MeDIP enrichments covering rare gene promoters (see below) and intergenic regions. It is noteworthy we could not validate the presence of 5-methylcytosine (5mC) by bisulfite sequencing in E3.5 blastocysts at several intergenic regions (data not shown), and we speculate that this represents nonspecific binding of the antibody in the absence of sufficient 5mC targets.

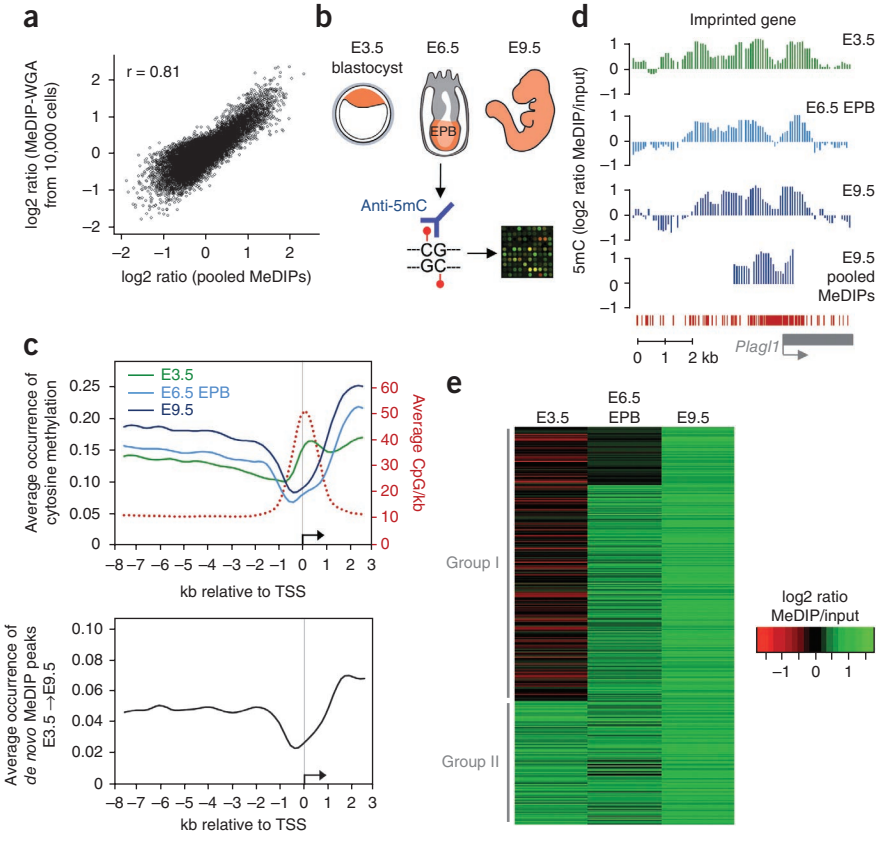

Figure 1 Profiling of DNA methylation during early mouse embryogenesis. (**a**) Comparison of MeDIP-WGA on 150 ng of DNA and of pooled unamplified MeDIPs on 2 μg of the same DNA (**Supplementary Fig. 1**). The scatter plot compares average log2 ratios in −400 bp to +400 bp relative to all TSS. (**b**) We hybridized MeDIP samples from E3.5 blastocysts, E6.5 epiblasts (EPB) and total E9.5 embryos on NimbleGen HD2 arrays covering 11 kb of all mouse promoters. (**c**) The top graph shows the fraction of tiles with a methylated region as a function of the distance to the TSS (black arrow). For comparison, the average CpG count per kilobase along the tiles is shown (red dotted line, right axis). The bottom graph shows the fraction of tiles with a *de novo* methylation peak as a function of the distance to the TSS. (**d**) MeDIP profiles at the imprinted gene *Plagl1* confirm the presence of a germline methylation mark[47]. The graphs show smoothed MeDIP over input ratios of individual oligonucleotides. Here and in all figures, the MeDIP profiles we obtained with unamplified pooled MeDIPs at E9.5 are also shown for validation. The gene is shown below the graphs as a gray box, and the transcription start site is shown as a gray arrow. Red bars represent the position of the CpGs. (**e**) The Heatmap shows the dynamics of DNA methylation at 691 genes with a methylated promoter in E9.5 embryos. Group I genes are *de novo* methylated in early embryos, whereas group II genes are already hypermethylated in preimplantation blastocysts.

Next we identified sites of *de novo* methylation during early development. *De novo* methylation is frequent in intergenic and intragenic regions but also occurs in gene promoters (**Fig. 1c**). Indeed, there are an increasing number of methylated promoters at consecutive stages of development, with rare demethylation events (**Supplementary Fig. 2c**). We identified 691 validated genes with a methylated promoter in E9.5 embryos, including 280 LCPs, 352 ICPs and 59 HCPs (**Supplementary Table 1**). LCPs and ICPs are highly over-represented among these genes ($P < 2.2 \times 10^{-16}$, Wilcoxon test), which confirms our observation that they are primary targets for DNA methylation[9,13]. We sorted these genes into two groups: group I genes ($n = 476$) are unmethylated in E3.5 blastocysts and gain promoter DNA methylation during early development, whereas group II genes ($n = 215$) show promoter DNA methylation throughout early development (**Fig. 1e**). Both groups show a similar distribution of promoter classes (**Table 1**; $P = 0.39$, χ^2 test), indicating that they are not discriminated by promoter CpG content.

Table 1 Functional annotation of genes with hypermethylated promoters in early mouse embryos

	Promoter classes						
	LCP	ICP	HCP	Tissue of expression	*P*	Enriched ontology terms	*P*
Group I	196	244	36	Testis	4.0×10^{-6}	Gamete generation	1.5×10^{-3}
$n = 476$				Egg	2.0×10^{-2}	Sexual reproduction	6.0×10^{-4}
						Defense response	4.9×10^{-3}
Group II $n = 215$	84	108	23	Testis	5.6×10^{-5}	Gamete generation	1.3×10^{-3}
						Sexual reproduction	1.3×10^{-3}

The table shows promoter classes and functional annotations associated with genes in group I ($n = 476$) and group II ($n = 215$). Both groups showed a similar distribution of promoter CpG content and are enriched for promoters with low or intermediate CpG content. To reveal functional annotations, the DAVID tool[49] was used by comparing genes in group I and II with all genes present on the array. For group I, only ICP and HCP genes were considered. The table shows the preferential tissues of expression and enriched ontology terms with associated Fisher exact *P* values calculated using the DAVID tool.

De novo CpG island methylation marks the epiblast stage

Most genes in group I gain promoter methylation in E6.5 epiblast and very few gain it in E9.5 embryos (**Fig. 1e**), indicating that the major step of promoter *de novo* methylation occurs during implantation in epiblast cells. Group I includes several pluripotency genes, which confirms that they are primary targets for promoter methylation during development[11,13]. The *Tcl1* promoter is *de novo* methylated in the epiblast (**Fig. 2a**), whereas the promoters of *Zfp42* (also known as *Rex1*), *Dppa3* (also known as *Stella*) and *Gdf3* are *de novo* methylated in E9.5 embryos (**Supplementary Fig. 4a**,**b**). We validated the timing of *de novo* methylation at the *Zfp42* and *Dppa3* promoters by COBRA (combined bisulfite restriction analysis) (**Supplementary Fig. 4c**). We also confirmed that *Elf5*, which encodes a trophoblast-specific transcription factor whose promoter methylation has been proposed to restrict differentiation of embryonic cells[27], is *de novo* methylated in epiblast cells (**Supplementary Fig. 4d**).

Because increasing evidence suggest that DNA methylation at LCPs is constitutive and can be bypassed by activating signals[9,12,28,29], we focused our analysis on CpG islands (present in ICPs and HCPs). We performed an ontology analysis that revealed a strong enrichment for genes expressed in both the male and female germline (**Table 1**). Examples include *Dazl*, *Prss21* (also known as *Testisin*), *Asz1*, *Mei1*, *Papolb* (also known as *Tpap*), *Tcam1*, *Brdt*, *Spo11*, and *Sycp1*, *Sycp3*, *Syce1* and *Tex12*, which encode synaptonemal complex components (**Fig. 2b** and **Supplementary Fig. 5**). Examples of genes specific to oocytes are *Nlrp5* (also known as

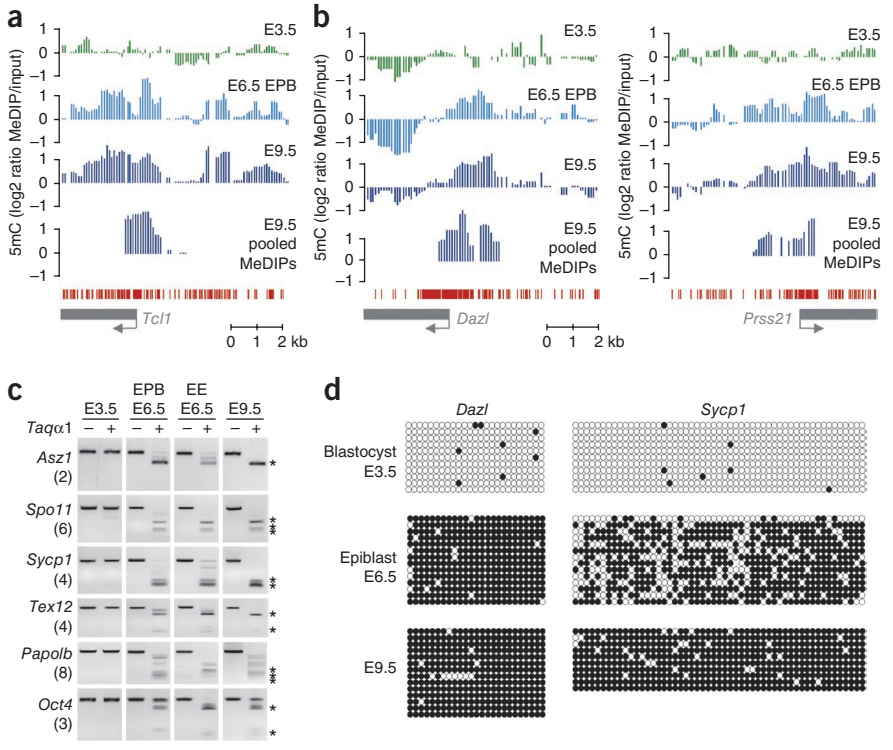

Figure 2 *De novo* CpG island methylation in epiblast cells. (**a**) *De novo* methylation of the pluripotency gene *Tcl1* in epiblast (EPB) cells. Other examples of *de novo* methylated pluripotency genes are given in **Supplementary Figure 4**. The graphs show smoothed MeDIP over input ratios of individual oligonucleotides. Red bars represent the position of CpGs. (**b**) Examples of germline-specific genes *de novo* methylated during implantation in epiblast cells. More examples are given in **Supplementary Figure 5**. (**c**) Validation of promoter DNA methylation by COBRA. All five tested germline-specific genes are *de novo* methylated at E6.5 in the EPB and the extraembryonic ectoderm (EE). The promoter of *Oct4*, which has been shown to be methylated in extraembryonic lineages[48] and partially *de novo* methylated in E9.5 embryos[38], is used as a control. Here and in all figures, the number of *Taq*αI sites in the amplified fragment is indicated in parenthesis, and asterisks mark restriction fragments representing end products of the digestion. (**d**) Bisulfite sequencing in the promoters of *Dazl* and *Sycp1* confirms *de novo* methylation during implantation in epiblast cells. Other validations by bisulfite sequencing are shown in **Supplementary Figure 7**. Circles represent CpG dinucleotides either unmethylated (open) or methylated (closed).

Nalp5 and *Mater*), *Bcl2l10* and NM_175017 (**Supplementary Fig. 5**). Validations by COBRA and HpaII digestion confirmed that these CpG-island promoters are unmethylated in E3.5 blastocysts but are hypermethylated in E6.5 epiblasts and E9.5 embryos (**Fig. 2c** and **Supplementary Fig. 6**). These promoters also gain substantial DNA methylation in the extraembryonic ectoderm at E6.5 (**Fig. 2c** and **Supplementary Fig. 6**). We performed bisulfite sequencing on four germline genes (*Dazl*, *Prss21*, *Tex12* and *Sycp1*), which confirmed that *de novo* CpG island methylation has already occurred in E6.5 epiblast (**Fig. 2d** and **Supplementary Fig. 7**). These genes are mostly unmethylated in E4.5 blastocysts (data not shown), indicating that *de novo* methylation is initiated during or after implantation. We conclude that the postimplantation epiblast acquires a distinct promoter methylation signature *in vivo*, in particular with the methylation of a large number of germline genes.

Reversible methylation during eye and hematopoietic development

Notably, group I also contains genes specific to differentiated tissues, which are mostly associated with ICP promoters. These include genes expressed in brain and eye (*Mbp, Pcdhb* genes, *Cryaa*, *Cryga-e* genes, and *Cplx4*; **Supplementary Fig. 8a**), many of which are members of gene family clusters or gain DNA methylation at alternative promoters. Striking examples are provided by the protocadherin loci (at *Pcdha* and *Pcdhg*) that gain DNA methylation at multiple alternative gene starts in E9.5 embryos (**Supplementary Fig. 9**). COBRA at the promoter of the eye-specific genes *Cplx4* and *Cryaa* confirms gain of DNA methylation in E6.5 epiblast as well as in extraembryonic ectoderm (**Supplementary Fig. 8b**). This is unexpected because elevated density of cytosine methylation is believed to be stably maintained and incompatible with subsequent expression in the eye. To test the possibility that promoter DNA methylation is reversible during somatic differentiation, we measured DNA methylation in the retina and lens and showed that promoter methylation is erased in a cell-type–specific way during eye development (**Supplementary Fig. 8b**).

Notably, we also observed that several promoters of hematopoietic genes (ontology term 'defense response'; **Table 1**) are *de novo* methylated during implantation, including *Pou2af1* (also known as *Obf1*), encoding a transcriptional coactivator involved in B-cell development, *Cytip* (also known as *Pscdbp*), a gene expressed in leukocytes, the toll-like receptors *Tlr1* and *Tlr6*, *Cxcl9*, *Gzmk*, *Abcg3* and *Niacr1* (also known as *pr109a*) (**Fig. 3a** and data not shown). COBRA of the promoters of *Pou2af1*, *Cytip* and *Tlr6* confirmed gain of DNA methylation in E6.5 epiblast and extraembryonic ectoderm (**Fig. 3b**). To test if these genes are demethylated during hematopoietic differentiation, we measured promoter methylation in hematopoietic progenitors, B cells and T cells. *Tlr6* and *Cytip* promoter methylation is abundant in hematopoietic progenitors isolated from E10.5 embryos and is subsequently erased in the hematopoietic lineage, whereas the B-cell–specific gene *Pou2af1* is specifically demethylated during differentiation of adult hematopoietic stem cells into B cells (**Fig. 3b**). We conclude that promoter DNA methylation acquired in epiblast can be reversed during terminal differentiation, which provides examples of demethylation at promoters with moderate CpG richness during somatic development.

Inheritance of promoter methylation from parental gametes

Group II genes show promoter methylation already present in preimplantation embryos (**Fig. 1e**). As could be expected, this group includes imprinted genes with a germline DMR near the TSS (**Fig. 1d** and **Supplementary Fig. 3**); however, we also identified many other genes not reported as imprinted. The ontology analysis revealed that group II is enriched in genes expressed in the male germline (**Table 1**). Selected ICP and HCP examples are *Piwil1* (also known as *Miwi*), *Csnka2ip* (also known as *Ckt2*), *Dpep3*, *Hdhd1a*, *Tssk2*, *Spaca4*, *Tuba3a* (also known as *Tuba3*) and *Gykl1* (**Fig. 4a** and **Supplementary Fig. 10a**). Group II also contains somatic genes expressed in hematopoietic cells (*Cd4* and *Fyb*) or retina (*Rrh*) (**Fig. 4a** and **Supplementary Fig. 10b**). Validations by COBRA indicated that all tested promoters are methylated in E6.5 epiblast, E6.5 extraembryonic ectoderm and E9.5 embryos but show a mixture of methylated and unmethylated alleles in E3.5 blastocysts (**Fig. 4b**). HpaII digestion confirmed partial promoter methylation of *Tuba3a*

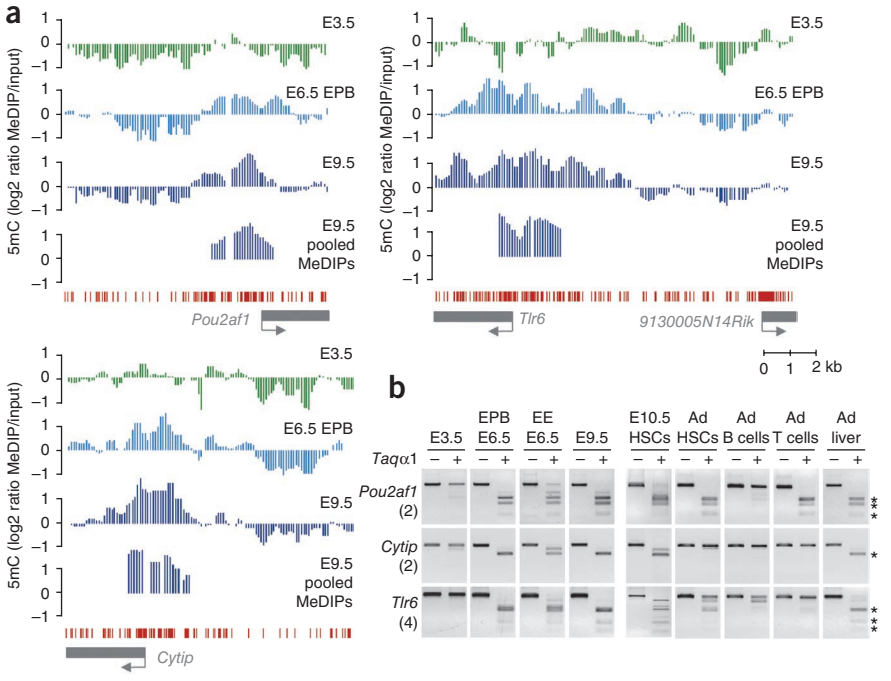

Figure 3 Promoter DNA methylation at hematopoietic genes is erased during hematopoietic differentiation. (**a**) The hematopoietic genes *Pou2af1*, *Tlr6* and *Cytip* gain promoter DNA methylation in EPB cells. The graphs show smoothed MeDIP over input ratios of individual oligonucleotides. Red bars represent the position of CpGs. (**b**) Validation by COBRA confirms that all three tested hematopoietic genes gain promoter DNA methylation during implantation and are hypermethylated at E6.5 in the EPB, the EE and in E9.5 embryos. All genes also show substantial promoter DNA methylation in hematopoietic stem cells (HSCs) isolated from E10.5 embryos. Subsequently in adults (Ad), *Cytip* and *Tlr6* promoter methylation is lost in bone marrow HSCs, B cells and T cells but is maintained in other tissues such as liver. For the B-cell–specific gene *Pou2af1*, promoter methylation is specifically erased during differentiation of adult HSCs into B cells.

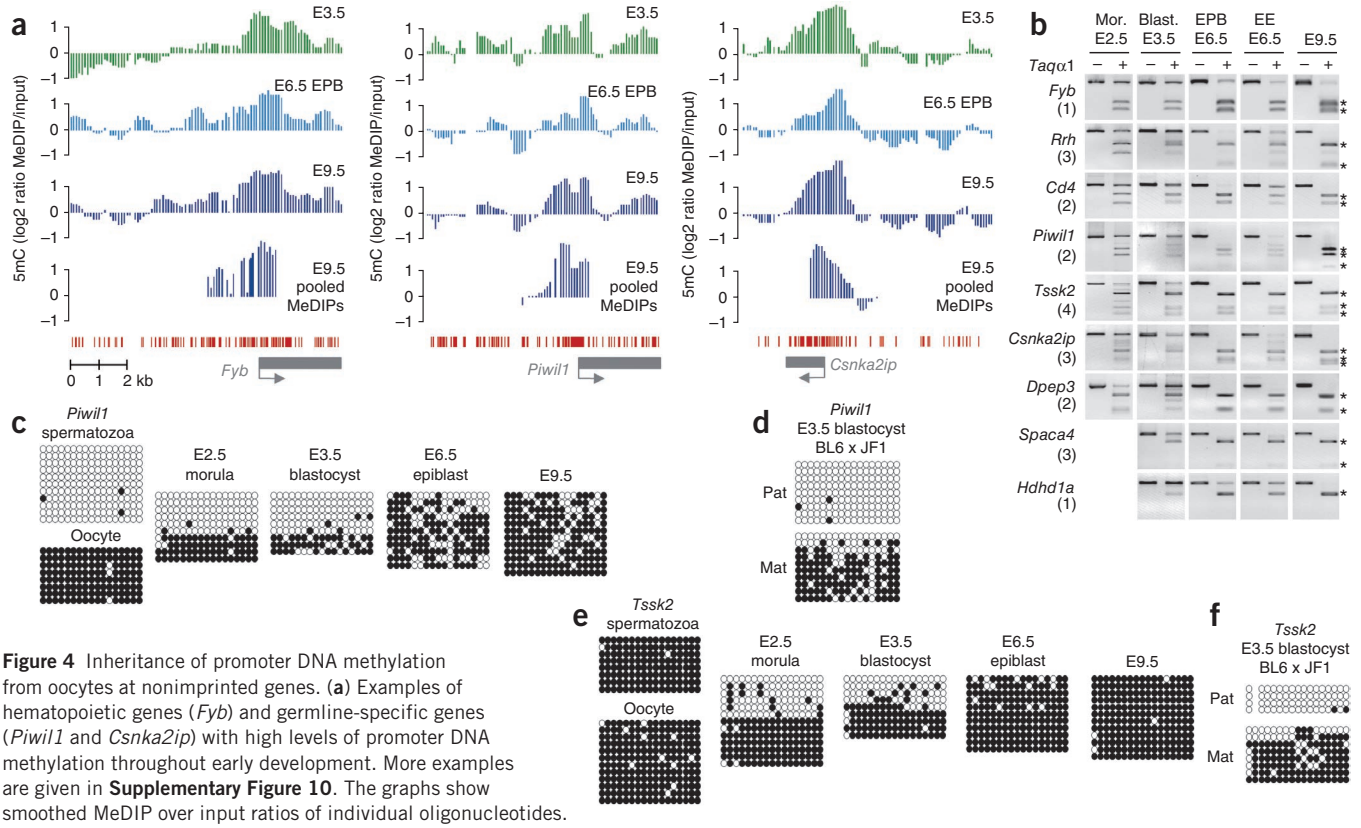

Figure 4 Inheritance of promoter DNA methylation from oocytes at nonimprinted genes. (**a**) Examples of hematopoietic genes (*Fyb*) and germline-specific genes (*Piwil1* and *Csnka2ip*) with high levels of promoter DNA methylation throughout early development. More examples are given in **Supplementary Figure 10**. The graphs show smoothed MeDIP over input ratios of individual oligonucleotides. Red bars represent the position of CpGs. (**b**) Validation of promoter DNA methylation by COBRA. All tested genes show hypermethylation in EPB and EE in E6.5 embryos. E3.5 blastocysts and E2.5 morulas show a consistent pattern of mixed methylated and unmethylated alleles. (**c**) Bisulfite sequencing in the promoter of *Piwil1* in gametes and early embryos. (**d**) Bisulfite sequencing in the *Piwil1* promoter in BL6 × JF1 E3.5 blastocysts shows that only maternal alleles carry DNA methylation. Mat, maternal alleles; pat, paternal alleles. (**e**) Bisulfite sequencing in the promoter of *Tssk2* in gametes and early embryos. (**f**) Bisulfite sequencing in the *Tssk2* promoter in BL6 × JF1 E3.5 blastocysts shows that only maternal alleles carry DNA methylation. Circles represent CpG dinucleotides either unmethylated (open) or methylated (closed).

and *Dpep3* in E3.5 blastocysts (**Supplementary Fig. 6**). To test if these genes are *de novo* methylated in blastocysts or whether they potentially inherit DNA methylation from gametes, we performed COBRA on E2.5 morulas. All tested genes (seven out of seven) showed methylated alleles in E2.5 morulas (**Fig. 4b**), suggesting that most genes in group II inherit methylated alleles from gametes. Next, we performed bisulfite sequencing in the promoters of *Piwil1*, *Dpep3*, *Csnka2ip*, *Tssk2*, *Spaca4*, *Rrh* and *Cd4* in gametes and early embryos. *Piwil1*, *Dpep3* and *Csnka2ip* promoters are methylated in oocytes but not in spermatozoa, are partially methylated in morulas and blastocysts and are fully methylated in epiblast and E9.5 embryos (**Fig. 4c** and **Supplementary Fig. 11a**,**b**), suggesting that they inherit methylation from oocytes whereas paternal alleles are methylated during implantation. To test this hypothesis, we used polymorphisms between BL6 and JF1 mice in the *Piwil1* promoter (no polymorphisms were found in *Dpep3* or *Csnka2ip*) and showed that methylated alleles in BL6 × JF1 E3.5 blastocysts are maternal (**Fig. 4d**). In contrast, *Tssk2*, *Spaca4*, *Rrh* and *Cd4* are methylated in both gametes but only partially in preimplantation embryos (**Fig. 4e** and **Supplementary Fig. 11c–e**), suggesting incomplete maintenance of methylation after fertilization, perhaps on one parental allele only. In support of this, polymorphisms in BL6 × JF1 E3.5 blastocysts showed that predominantly maternal *Tssk2* and *Spaca4* alleles retained DNA methylation (**Fig. 4f** and **Supplementary Fig. 11c**). This identifies nonimprinted sequences that resist global DNA methylation reprogramming during preimplantation development.

De novo DNA methylation by Dnmt3B maintains gene repression

The *de novo* methyltransferases Dnmt3a and Dnmt3b display different expression patterns and target specificities[30,31]. To determine which enzyme is responsible for *de novo* methylation in early development, we measured DNA methylation in *Dnmt3a*$^{-/-}$ and *Dnmt3b*$^{-/-}$ E9.5 embryos. COBRA and bisulfite sequencing showed that germline-specific genes are severely hypomethylated in the absence of Dnmt3b but not of Dnmt3a (**Fig. 5a** and **Supplementary Fig. 12**). DNA methylation at pluripotency genes, hematopoietic genes and eye genes is also markedly reduced in *Dnmt3b*$^{-/-}$ but not *Dnmt3a*$^{-/-}$ E9.5 embryos (**Fig. 5b**). This shows that Dnmt3b is the main enzyme required for promoter *de novo* methylation during implantation. Notably, DNA methylation at certain genes such as *Brdt*, *Dpep3*, *Cytip* and *Crygd* is only partially reduced in *Dnmt3b*$^{-/-}$ embryos (**Fig. 5a**,**b** and **Supplementary Fig. 12c**,**d**), suggesting that Dnmt3a cooperates with Dnmt3b to methylate these targets. To further assess the function of promoter DNA methylation, we measured the expression of several target genes by RT-qPCR in wildtype and mutant E9.5 embryos. Although all genes were barely detectable in wildtype and *Dnmt3a*$^{-/-}$ embryos, hypomethylation in *Dnmt3b*$^{-/-}$ embryos was associated with a 13–50-fold reactivation at most germline genes and one pluripotency gene (*Zfp42*), showing that somatic DNA methylation is required for stable gene repression (**Fig. 5c**). Other tested genes, including the hematopoietic genes *Pou2af1* and *Tlr6*, were not reactivated despite promoter hypomethylation in *Dnmt3b*$^{-/-}$ embryos (**Fig. 5c**), indicating that absence of DNA methylation is not sufficient to promote

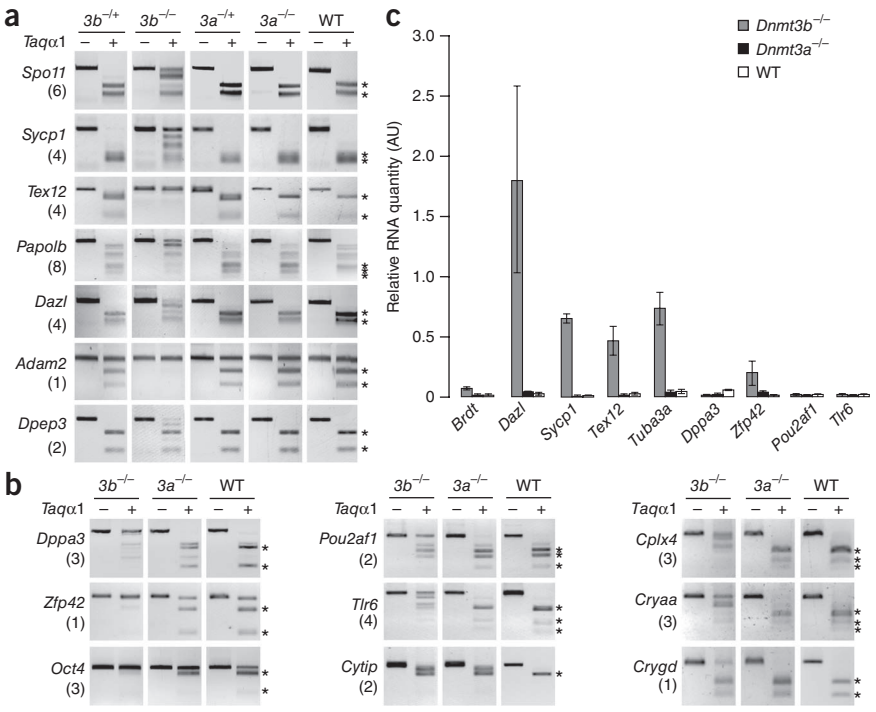

Figure 5 Promoter DNA methylation mediated by Dnmt3b maintains gene repression *in vivo*. (**a**) DNA methylation in the promoter of the indicated germline-specific genes was analyzed by COBRA in wildtype (WT) and mutant E9.5 embryos heterozygous or homozygous for *Dnmt3* deletions. Most tested genes showed severe reduction of promoter DNA methylation in *Dnmt3b*$^{-/-}$ embryos but were unaffected in *Dnmt3a*$^{-/-}$ embryos. Additional validations by bisulfite sequencing are shown in **Supplementary Figure 12**. (**b**) Promoter DNA methylation by COBRA in wildtype and *Dnmt3* mutant E9.5 embryos at pluripotency genes (left), hematopoietic genes (middle) and eye genes (right). (**c**) Absence of promoter *de novo* methylation is associated with gene reactivation. Expression of indicated genes was measured by real-time qPCR in wildtype (WT), *Dnmt3a*$^{-/-}$ and *Dnmt3b*$^{-/-}$ E9.5 embryos. Values are arbitrary units after normalization to three housekeeping genes (*Gapdh*, *Rpl13A* and *Actb*). Error bars represent standard deviations from two or three independent experiments.

gene transcription, which probably reflects the absence of suitable transcription factors at this developmental stage. Altogether, this demonstrates that promoter DNA methylation is primarily mediated by Dnmt3b and maintains gene silencing in developing embryos *in vivo*.

Comparison of DNA methylation in embryonic stem cells and early embryos

Embryonic stem cells are derived from the inner cell mass of preimplantation blastocysts; however, it is unclear to what *in vivo* cellular population they are most related[32]. Thus, we asked how promoter methylation in early embryos compares with promoter methylation in embryonic stem cells differentiating into neurons[13]. First, we show that most promoters methylated in neuronal progenitors are hypomethylated in total embryos (**Supplementary Fig. 13a**), which reflects DNA methylation specific to cells committed to the neuronal lineage. Targets that gain promoter methylation in both neuronal progenitors and total embryos include several pluripotency genes (*Tcl1*, *Gdf3*, *Zfp42* and *Dppa3*). Next, we focused on gene promoters hypermethylated in embryonic stem cells. Out of 675 gene promoters methylated in embryonic stem cells, only 38% (255 out of 675) were also enriched in E3.5 blastocysts (**Supplementary Fig. 13b**,**c**). These were mainly genes from group II that show high levels of DNA methylation throughout early development (including *Dpep3*, *Piwil1*, *Spaca4*, *Tssk2*, *Tuba3a*, *Fyb*, *Rrh* and *Cd4*). Many genes hypermethylated in embryonic stem cells are the ones that also gain methylation in postimplantation embryos (that is, the germline-specific genes *Dazl*, *Prss21*, *Sycp1*, *Spo11* and *Tex12*, the hematopoietic genes *Pou2af1*, *Cytip*, *Tlr1* and *Niacr1* (also known as *Gpr109a*) and the eye genes *Cplx4* and *Cryaa*). Consequently, 69% (463 out of 675) of the promoters hypermethylated in embryonic stem cells are also methylated in E6.5 epiblasts and 85% (572 out of 675) are also methylated in E9.5 embryos (**Supplementary Fig. 13b**,**c**). This comparison also highlights that many *de novo* methylation targets identified in this study could not be identified in studies of differentiating embryonic stem cells. Finally, a minor group of gene promoters (71 out of 675) methylated in embryonic stem cells are never methylated in embryos (**Supplementary Fig. 13b**), which might reflect abnormal DNA methylation induced by culture conditions or strain differences. Altogether, this indicates that during derivation and culture, embryonic stem cells accumulate promoter DNA methylation that occurs during and after implantation *in vivo*. Consequently, cultured embryonic stem cells bear a promoter DNA methylation signature that resembles that of postimplantation embryos.

DISCUSSION

We used an optimized MeDIP protocol to reveal that the major step of gene methylation occurs during implantation in epiblast cells, which coincides with *de novo* methylation observed by immunofluorescence[7]. Notably, this correlates with a reduction in cellular potency, highlighted by the fact that postimplantation epiblast stem cells (EpiSCs) rarely contribute to chimeras[33,34], suggesting that DNA methylation constitutes an epigenetic boundary that limits the potency of epiblast cells. The reduced potency of EpiSCs could also be explained by abnormal DNA methylation during derivation and culture, as exemplified by the pluripotency genes *Dppa3* and *Zfp42* that are methylated in EpiSCs but not in epiblast *in vivo*[35]. Similarly, we show that embryonic stem cells adopt a promoter methylation signature that resembles that of postimplantation embryos rather than the blastocysts from which they are derived. This is in line with recent data showing that derivation of embryonic stem cells induces changes in H3K4 and H3K27 methylation[36]. The impact of these epigenetic differences can be put into question because embryonic stem cells are still able to contribute to all germ layers when reintroduced into blastocysts and share similar properties with naïve epiblast cells from mature blastocysts[32]. It is possible that this reflects a strong heterogeneity between embryonic stem cells[37] or that DNA methylation is reversed when cells are placed back in an *in vivo* environment. We also note that in contrast to EpiSCs, DNA methylation in embryonic stem cells does not target pluripotency genes, which might explain why it does not impact their development potential.

Immunostaining experiments have shown that DNA methylation is reduced in extraembryonic as compared to embryonic lineages[7],

a difference that is persistent because the placenta is hypomethylated compared to the embryo proper[23]. Interestingly, this difference is not evident at the level of promoters. Our data show that most genes tested gain promoter DNA methylation equally in epiblast and extraembryonic ectoderm at E6.5, although we note a slightly reduced methylation in the extraembryonic ectoderm at some genes (*Pou2af1*, *Cplx4*, *Cryaa* and *Cd4*). This is in line with a previous study's results showing similar promoter methylation between cultured embryonic stem and trophoblast stem cells[11]. Therefore, CpG island methylation does not follow global DNA methylation patterns, which might indicate that they are under the control of different pathways.

Few genes have been shown to require DNA methylation for correct spatiotemporal expression *in vivo*. Rare examples include *Oct4* and *Nanog* (ref. 38), as well as the *Rhox* genes[16]. Our data reveals that one important function of DNA methylation is to repress the germline expression program in developing embryos *in vivo*. Previous studies have identified germline-specific genes as targets of CpG island methylation in differentiated cells[9,10,39,40]. Here we identify many new targets and extend these observations by showing that methylation occurs during implantation before organogenesis and is required to maintain gene silencing *in vivo*. It is remarkable that some of these genes show high concentrations of CpGs in their promoters (more than four CpGs per 100 bp), a feature that is otherwise associated with hypomethylation in the genome, except at germline DMRs in imprinted loci. This strongly suggests the existence of mechanisms that specifically recruit DNA methylation to germline genes[40]. We speculate that this methylation does not initiate gene silencing but rather acts as a locking system to prevent deleterious effects caused by ectopic reactivation in somatic cells. Two arguments support this model. First, germline genes acquire DNA methylation during implantation when they are already silent. Second, many of these genes are overexpressed in cancer, which suggests that their ectopic reactivation negatively impacts somatic cellular integrity[41].

Surprisingly, other targets of promoter methylation in early embryos are genes programmed to be expressed later during development, in particular in the hematopoietic and neuronal lineages. By studying these targets, we made two unexpected observations. First, several targets are members of gene family clusters (the *Cryg* cluster, the *Cxcl* cluster, *protocadherin* loci and the *Tlr1–6* cluster), which suggests that DNA methylation might have evolved as a mechanism to regulate duplicated promoters. Second, promoter methylation acquired in epiblast is erased during terminal differentiation. To date, very few examples of promoter demethylation have been described *in vivo*, mostly at very CpG-poor promoters[42]. This demethylation is possibly a consequence of gene activation, as shown recently for the hormone-response genes *TFF1* (ref. 29) and *CYP27B1* (ref. 28). Here we report demethylation at promoters with higher CpG richness, and further studies are required to test if this is a consequence of gene activation and what mechanisms are involved. This observation contradicts the model whereby loss of differentiation potential during development is associated with increased promoter DNA methylation. In contrast, it suggests that reversible DNA methylation restrains the early expression of key differentiation genes, a function similar to polycomb-mediated H3K27 in pluripotent cells[43,44]. This model predicts that absence of DNA methylation leads to early gene activation during development. So far, we have not been able to demonstrate reactivation of hematopoietic genes in *Dnmt3b*$^{-/-}$ E9.5 embryos; however, further studies at other targets and developmental stages are necessary to clarify this issue.

Our results show that Dnmt3b is the main enzyme responsible for *de novo* methylation at tested genes in early embryos. This is compatible with studies showing that Dnmt3b is detected in preimplantation embryos and epiblast, whereas Dnmt3a is more prevalent in late embryos[31,45]. However, rare genes (*Brdt*, *Dpep3*, *Cytip* and *Crygd*) only show minor or partial reduction of methylation in absence of Dnmt3b or Dnmt3a, suggesting that both enzymes cooperate at these targets. This is in line with studies showing a synergistic action of Dnmt3a and Dnmt3b at *Oct4*, *Nanog* and *Rhox* in E8.5–E9.5 embryos[16,38]. This indicates that different genomic regions show different specificities for Dnmt3 enzymes. In the future, efforts should be concentrated on understanding the mechanisms that recruit Dnmt3 enzymes to their targets.

Finally, we reveal that certain genes, in particular germline genes but also somatic genes, resist global demethylation after fertilization and inherit promoter DNA methylation from parental gametes. So far, all tested genes indicate that post-fertilization inheritance of DNA methylation occurs from oocytes; however, additional validations are required to test if it also occurs from spermatozoa. These genes differ from imprinted genes because some are methylated in both gametes, and none of these genes maintains allele-specific methylation after implantation. At the condition that these genes are not transiently demethylated at a specific developmental stage, this suggests that there is transgenerational transmission of DNA methylation at a substantial fraction of the genome. It will be important to test whether similar mechanisms maintain DNA methylation at imprinted genes and germline genes, and whether specific sequence elements confer resistance to epigenetic reprogramming. Together with recent work showing that histone modifications are transmitted from the gametes to the embryo[20,21], this indicates that fertilization involves the transmission of epigenetic information that might be important to guide the early steps of development. In addition, by showing that transgenerational transmission of DNA methylation can occur at nonimprinted sequences in mammals, our results justify the search for transmission of altered DNA methylation that is linked to environmental factors[46].

URLs. R software for statistical computing, http://www.r-project.org/; DAVID functional annotation tool, http://david.abcc.ncifcrf.gov/; UCSC Genome Annotation, http://www.genome.ucsc.edu/; MethPrimer software, http://www.urogene.org/methprimer/index1.html.

METHODS

Methods and any associated references are available in the online version of the paper at http://www.nature.com/naturegenetics/.

Accession codes. Microarray data are accessible from the GEO database under accession code GSE22831.

Note: Supplementary information is available on the Nature Genetics website.

ACKNOWLEDGMENTS

We thank R. Vicente for assistance with the flow cytometry, T. Gostan for help with R programming, and E. Posfai and R. Hirasawa for advice on embryo dissection. This research was supported by the Epigenome NoE (LSHG-CT-2006-037415), Novartis Research Foundation, Centre National de la Recherche Scientifique (CNRS), Agence Nationale de la Recherche (ANR-07-BLAN-0052-02), Association pour la Recherche sur le Cancer (ARC contract 4868) and European Chemical Industry Council (CEFIC) Long Research Initiative (LRI-EMSG49-CNRS-08).

AUTHOR CONTRIBUTIONS

J.B. performed all experiments and data analysis and contributed to the writing of the manuscript. S.G. developed R scripts and participated in data analysis. Y.L., H.C. and H.S. prepared samples from *Dnmt* mutant embryos. D.S. and T.F. participated in the study design and writing of the manuscript. M.W. designed and supervised the study, participated in data analysis and wrote the manuscript.

COMPETING FINANCIAL INTERESTS
The authors declare no competing financial interests.

Published online at http://www.nature.com/naturegenetics/.
Reprints and permissions information is available online at http://npg.nature.com/reprintsandpermissions/.

1. Reik, W. Stability and flexibility of epigenetic gene regulation in mammalian development. *Nature* **447**, 425–432 (2007).
2. Lei, H. *et al. De novo* DNA cytosine methyltransferase activities in mouse embryonic stem cells. *Development* **122**, 3195–3205 (1996).
3. Okano, M., Bell, D.W., Haber, D.A. & Li, E. DNA methyltransferases Dnmt3a and Dnmt3b are essential for *de novo* methylation and mammalian development. *Cell* **99**, 247–257 (1999).
4. Mayer, W., Niveleau, A., Walter, J., Fundele, R. & Haaf, T. Demethylation of the zygotic paternal genome. *Nature* **403**, 501–502 (2000).
5. Oswald, J. *et al.* Active demethylation of the paternal genome in the mouse zygote. *Curr. Biol.* **10**, 475–478 (2000).
6. Rougier, N. *et al.* Chromosome methylation patterns during mammalian preimplantation development. *Genes Dev.* **12**, 2108–2113 (1998).
7. Dean, W. *et al.* Conservation of methylation reprogramming in mammalian development: aberrant reprogramming in cloned embryos. *Proc. Natl. Acad. Sci. USA* **98**, 13734–13738 (2001).
8. Illingworth, R. *et al.* A novel CpG island set identifies tissue-specific methylation at developmental gene loci. *PLoS Biol.* **6**, e22 (2008).
9. Weber, M. *et al.* Distribution, silencing potential and evolutionary impact of promoter DNA methylation in the human genome. *Nat. Genet.* **39**, 457–466 (2007).
10. Shen, L. *et al.* Genome-wide profiling of DNA methylation reveals a class of normally methylated CpG island promoters. *PLoS Genet.* **3**, 2023–2036 (2007).
11. Farthing, C.R. *et al.* Global mapping of DNA methylation in mouse promoters reveals epigenetic reprogramming of pluripotency genes. *PLoS Genet.* **4**, e1000116 (2008).
12. Meissner, A. *et al.* Genome-scale DNA methylation maps of pluripotent and differentiated cells. *Nature* **454**, 766–770 (2008).
13. Mohn, F. *et al.* Lineage-specific polycomb targets and *de novo* DNA methylation define restriction and potential of neuronal progenitors. *Mol. Cell* **30**, 755–766 (2008).
14. Bhutani, N. *et al.* Reprogramming towards pluripotency requires AID-dependent DNA demethylation. *Nature* **463**, 1042–1047 (2009).
15. Mikkelsen, T.S. *et al.* Dissecting direct reprogramming through integrative genomic analysis. *Nature* **454**, 49–55 (2008).
16. Oda, M. *et al.* DNA methylation regulates long-range gene silencing of an X-linked homeobox gene cluster in a lineage-specific manner. *Genes Dev.* **20**, 3382–3394 (2006).
17. Brunner, A.L. *et al.* Distinct DNA methylation patterns characterize differentiated human embryonic stem cells and developing human fetal liver. *Genome Res.* **19**, 1044–1056 (2009).
18. Jirtle, R.L. & Skinner, M.K. Environmental epigenomics and disease susceptibility. *Nat. Rev. Genet.* **8**, 253–262 (2007).
19. Lane, N. *et al.* Resistance of IAPs to methylation reprogramming may provide a mechanism for epigenetic inheritance in the mouse. *Genesis* **35**, 88–93 (2003).
20. Hammoud, S.S. *et al.* Distinctive chromatin in human sperm packages genes for embryo development. *Nature* **460**, 473–478 (2009).
21. Puschendorf, M. *et al.* PRC1 and Suv39h specify parental asymmetry at constitutive heterochromatin in early mouse embryos. *Nat. Genet.* **40**, 411–420 (2008).
22. Lister, R. *et al.* Human DNA methylomes at base resolution show widespread epigenomic differences. *Nature* **462**, 315–322 (2009).
23. Popp, C. *et al.* Genome-wide erasure of DNA methylation in mouse primordial germ cells is affected by AID deficiency. *Nature* **463**, 1101–1105 (2010).
24. Weber, M. *et al.* Chromosome-wide and promoter-specific analyses identify sites of differential DNA methylation in normal and transformed human cells. *Nat. Genet.* **37**, 853–862 (2005).
25. Ball, M.P. *et al.* Targeted and genome-scale strategies reveal gene-body methylation signatures in human cells. *Nat. Biotechnol.* **27**, 361–368 (2009).
26. Laurent, L. *et al.* Dynamic changes in the human methylome during differentiation. *Genome Res.* **20**, 320–331 (2010).
27. Ng, R.K. *et al.* Epigenetic restriction of embryonic cell lineage fate by methylation of Elf5. *Nat. Cell Biol.* **10**, 1280–1290 (2008).
28. Kim, M.S. *et al.* DNA demethylation in hormone-induced transcriptional derepression. *Nature* **461**, 1007–1012 (2009).
29. Métivier, R. *et al.* Cyclical DNA methylation of a transcriptionally active promoter. *Nature* **452**, 45–50 (2008).
30. Kato, Y. *et al.* Role of the Dnmt3 family in *de novo* methylation of imprinted and repetitive sequences during male germ cell development in the mouse. *Hum. Mol. Genet.* **16**, 2272–2280 (2007).
31. Watanabe, D., Suetake, I., Tada, T. & Tajima, S. Stage- and cell-specific expression of Dnmt3a and Dnmt3b during embryogenesis. *Mech. Dev.* **118**, 187–190 (2002).
32. Nichols, J., Silva, J., Roode, M. & Smith, A. Suppression of Erk signaling promotes ground state pluripotency in the mouse embryo. *Development* **136**, 3215–3222 (2009).
33. Brons, I.G. *et al.* Derivation of pluripotent epiblast stem cells from mammalian embryos. *Nature* **448**, 191–195 (2007).
34. Tesar, P.J. *et al.* New cell lines from mouse epiblast share defining features with human embryonic stem cells. *Nature* **448**, 196–199 (2007).
35. Bao, S. *et al.* Epigenetic reversion of post-implantation epiblast to pluripotent embryonic stem cells. *Nature* **461**, 1292–1295 (2009).
36. Dahl, J.A., Reiner, A.H., Klungland, A., Wakayama, T. & Collas, P. Histone H3 lysine 27 methylation asymmetry on developmentally-regulated promoters distinguish the first two lineages in mouse preimplantation embryos. *PLoS ONE* **5**, e9150 (2010).
37. Hayashi, K., Lopes, S.M., Tang, F. & Surani, M.A. Dynamic equilibrium and heterogeneity of mouse pluripotent stem cells with distinct functional and epigenetic states. *Cell Stem Cell* **3**, 391–401 (2008).
38. Li, J.Y. *et al.* Synergistic function of DNA methyltransferases Dnmt3a and Dnmt3b in the methylation of Oct4 and Nanog. *Mol. Cell. Biol.* **27**, 8748–8759 (2007).
39. Maatouk, D.M. *et al.* DNA methylation is a primary mechanism for silencing postmigratory primordial germ cell genes in both germ cell and somatic cell lineages. *Development* **133**, 3411–3418 (2006).
40. Straussman, R. *et al.* Developmental programming of CpG island methylation profiles in the human genome. *Nat. Struct. Mol. Biol.* **16**, 564–571 (2009).
41. Simpson, A.J., Caballero, O.L., Jungbluth, A., Chen, Y.T. & Old, L.J. Cancer/testis antigens, gametogenesis and cancer. *Nat. Rev. Cancer* **5**, 615–625 (2005).
42. Waterland, R.A. *et al.* Epigenomic profiling indicates a role for DNA methylation in early postnatal liver development. *Hum. Mol. Genet.* **18**, 3026–3038 (2009).
43. Boyer, L.A. *et al.* Polycomb complexes repress developmental regulators in murine embryonic stem cells. *Nature* **441**, 349–353 (2006).
44. Lee, T.I. *et al.* Control of developmental regulators by Polycomb in human embryonic stem cells. *Cell* **125**, 301–313 (2006).
45. Hirasawa, R. *et al.* Maternal and zygotic Dnmt1 are necessary and sufficient for the maintenance of DNA methylation imprints during preimplantation development. *Genes Dev.* **22**, 1607–1616 (2008).
46. Skinner, M.K. & Guerrero-Bosagna, C. Environmental signals and transgenerational epigenetics. *Epigenomics* **1**, 111–117 (2009).
47. Smith, R.J. *et al.* The mouse Zac1 locus: basis for imprinting and comparison with human ZAC. *Gene* **292**, 101–112 (2002).
48. Hattori, N. *et al.* Epigenetic control of mouse Oct-4 gene expression in embryonic stem cells and trophoblast stem cells. *J. Biol. Chem.* **279**, 17063–17069 (2004).
49. Huang da, W., Sherman, B.T. & Lempicki, R.A. Systematic and integrative analysis of large gene lists using DAVID bioinformatics resources. *Nat. Protoc.* **4**, 44–57 (2009).

ONLINE METHODS

Isolation of cells and embryos. Embryos were obtained by natural breeding of C57BL/6 mice. The morning of the vaginal plug was designated E0.5. Embryos were dissected at E6.5 and E9.5 in M2 medium (Sigma-Aldrich). At E6.5, we separated the epiblast from the extraembryonic ectoderm and controlled for proper dissection using *Oct4* DNA methylation as a marker. Each MeDIP was performed on DNA from 30 pooled epiblasts. Blastocysts were collected at E3.5 by flushing the uteri with M2 medium. Each MeDIP was then performed on 300 pooled blastocysts. Morulas were collected at the 16–32 cell stage at E2.5 by flushing the oviducts with M2 medium. Grown oocytes were collected in M2 medium from dissected ovaries of 5-week-old females. The majority of oocytes were 60–80 mm in diameter. The presence of somatic contamination in the oocytes was eliminated by performing bisulfite sequencing in the *H19* DMR, which appeared hypomethylated (data not shown). To isolate hematopoietic stem cells (HSCs) from E10.5 embryos, we pooled aorta-gonad-mesonephros (AGMs) dissected from ten embryos and isolated $CD34^+$/c-Kit^+ cells by flow cytometry (FacsAria, BD Biosciences). To isolate adult HSCs, we collected bone marrow cells from femurs and tibias. We first isolated lineage negative (Lin–) cells by incubation with rat mouse antibodies directed against lineage markers (Ter119, B220, Mac-1, GR-1 and CD4) followed by anti-rat IgG magnetic beads, and then we isolated c-Kit^+/$Sca\text{-}1^+$/$B220^-$ HSCs from Lin– cells by flow cytometry. T cells and B cells were isolated by flow cytometry from adult lymph nodes as $CD4^+$/$CD8^+$/$CD3^+$ cells and $B220^+$/$CD19^+$ cells, respectively. We produced *Dnmt3* mutant embryos without oocyte-derived enzymes by crossing *Dnmt3a*$^{2lox/2lox}$; *Zp3*-Cre females, which conditionally delete *Dnmt3a* in growing oocytes, with *Dnmt3a*$^{+/-}$ males, and *Dnmt3b*$^{2lox/2lox}$; *Zp3*-Cre females with *Dnmt3b*$^{+/-}$ males[45].

MeDIP-on-ChiP. Sonication of DNA was performed with a Diagenode Bioruptor. MeDIP was performed as described[24], with adaptations. For unamplified MeDIP on 2 µg sonicated DNA, we used 2 µl of 5mC antibody (AbD Serotec, clone 33D3, 1 mg/ml) and 30 µl of M280 sheep anti-mouse IgG magnetic beads (Invitrogen). For MeDIP on low amounts of DNA, we sonicated 150 ng of DNA and used 1 µl 5mC antibody diluted 1/5 and 2 µl M280 magnetic beads in a final volume of 150 µl immunoprecipitation buffer. For E6.5 epiblasts and blastocysts, we used 1 µl 5mC antibody diluted 1/10 and 1/30 to account for the reduced global methylation. Subsequently, we amplified 5 ng input DNA and the entire MeDIP product with the Whole Genome Amplification kit (Sigma-Aldrich), following the manufacturer's instructions. MeDIP at E6.5 and E9.5 was done in triplicates, whereas MeDIP at E3.5 was done in duplicates because of the high number of blastocysts required. Amplified samples were hybridized to Roche NimbleGen HD2 2.1M Deluxe Promoter arrays, which contain 50–75 monomer oligonucleotides tiled in regions covering –8,200 bp to +3000 bp from 23,517 potential transcription start sites. Sample labeling and microarray hybridization were done according to standard procedure by Roche NimbleGen. Control unamplified MeDIP profiles at E9.5 (**Supplementary Fig. 1**) were generated by hybridizing 20 pooled unamplified MeDIPs (each generated from 2 µg of DNA) together with input DNA to Roche NimbleGen 385K RefSeq Promoter arrays.

Microarray analysis. Data processing and calculations were performed with the R computing software (see URLs). First, we calculated MeDIP/Input log2 ratios for each oligonucleotide from raw fluorescence values provided by Roche NimbleGen. All datasets were normalized using the loess method from the Limma package[50], which was modified to use input signal instead of total signal as a reference. We averaged normalized log2 ratios from biological replicates of the same embryonic stage, which showed good reproducibility ($r = 0.77$ and $r = 0.67$ with E9.5 embryos, $r = 0.60$ and $r = 0.58$ with E6.5 epiblasts, $r = 0.48$ with E3.5 blastocysts, $r = 0.78$ and $r = 0.79$ with pooled MeDIPs at E9.5). To compare microarray results from different samples, we normalized average log2 ratios to have identical normal distributions using the Limma package[50]. For data representation, we smoothed average log2 ratios over 400-bp windows using the Ringo package and created GFF files visualized with the SignalMap software (Roche NimbleGen). The promoter set on the array was filtered with UCSC Genome annotations to identify promoters with at least one RefSeq gene and one mRNA in the regions 200 bp upstream or downstream of the potential TSS, which identified 18,577 validated promoters. To determine promoter classes, we measured the GC content and the CpG ratio of observed to expected values in sliding 500-bp windows with a 5-bp offset in regions –900 bp to +400 bp relative to the TSS. Promoter classes were defined as follows: LCPs contain no 500-bp window with a CpG ratio >0.45; HCPs contain at least one 500-bp window with a CpG ratio >0.65 and GC content >55%; ICPs do not meet the previous criteria. To compare MeDIP-WGA and pooled MeDIPs at E9.5 that were performed on different array designs (**Fig. 1a**), we averaged log2 ratios in regions covering –400 to +400 bp relative to all TSS. To represent methylation along tiled regions (**Fig. 1c**), we calculated the fraction of tiles with a methylated region (defined as more than six consecutive oligos with a smoothed MeDIP ratio >0.25) and a *de novo* methylation peak (more than six consecutive oligos with a smoothed MeDIP ratio >0.5 in E9.5 embryos and less than six consecutive oligos with a smoothed MeDIP ratio >0.25 in E3.5 blastocysts) as a function of the distance to the TSS using the Ringo package. To find MeDIP peaks, we identified regions with more than six consecutive oligonucleotides with a smoothed log2 ratio >0.5 using the Ringo package. We defined genes with methylated promoters as genes with a MeDIP peak overlapping or less than 300 bp upstream of the TSS. In E9.5 embryos, this identified 691 validated promoters (411 ICPs and HCPs) after removal of duplicates, olfactory receptors, genes on the X chromosome and genes showing inconsistent profiles with pooled MeDIPs at E9.5. To generate **Figure 1e**, we averaged log2 ratios for all oligonucleotides located within the methylation peak identified in E9.5 embryos. The Heatmap was created using the gplots package. Group I genes had an average log2 ratio <0.3 in E3.5 and an average log2 ratio >0.3 in E9.5 embryos; group II genes had an average log2 ratio >0.3 in E3.5 and E9.5 embryos. The ontology analysis was performed with the DAVID functional annotation tool[49] by comparing group I and II genes versus all genes of the same promoter classes present on the array. For comparison with embryonic stem cells, we used data measuring the average MeDIP ratios in regions covering –700 bp to +200 bp relative to the TSS[13]. We defined hypermethylated promoters in embryonic stem cells with a log2 ratio >0.4. For a comparison with our data, we averaged oligonucleotide log2 ratios in the same region for all promoters that could be matched based on RefSeq annotations.

DNA methylation analysis by COBRA, bisulfite sequencing and HpaII digestion. For all samples except oocytes, we performed bisulfite conversion with the EpiTect kit (Qiagen) following DNA extraction by proteinase K digestion and phenol-chloroform extraction. For oocytes, we incubated 600 oocytes for 90 min at 37 °C in 32.5 µl 1 mM SDS, 280 µg/ml proteinase K and 10 µg glycogen, denatured at 50 °C for 15 min after addition of 1.1 µl NaOH 10 N and converted at 55 °C for 4 h after addition of 200 µl 4 M sodium bisulfite at pH 5.0, 1.5 µl 75 mM hydroquinone and 5 µg glycogen. Subsequent desulfonation of oocyte DNA was performed with the EpiTect kit. We used MethPrimer to design primers on bisulfite-treated DNA. PCR programs consisted of 20 cycles of touchdown PCR (62–52 °C, with a 0.5 °C decrease per cycle) followed by 30 cycles with annealing at 52 °C. For COBRA, we digested the PCR product with 10 U *Taqα1* for 1 h at 65 °C and used an equal amount of PCR product for the undigested control. For bisulfite sequencing, we cloned PCR fragments with the QIAGEN PCR cloning kit and removed clones with identical patterns of conversion. For HpaII experiments, we mixed 200 ng of DNA with 20U *Xba*I, 20U HindIII, restriction buffer, and split the mixture in equal amounts in three tubes containing 1 µl H_2O, 1 µl of HpaII 10 U/µl or 1µl *Msp*I 10 U/µl. Samples were incubated at 37 °C for 2 h, and we used 2 µl of the samples for qPCR quantification. Values given are the average of two or three independent experiments. Primers are given in **Supplementary Table 2**.

Expression analysis. Total RNA was treated with the RQ1 DNase according to the manufacturer's instructions. One microgram of total RNA was reverse transcribed with the First-Strand cDNA Synthesis Kit (GE Healthcare) using random primers. In parallel, we treated 1 µg of RNA without reverse transcription enzyme as a negative control. Quantifications were performed using real-time PCR and the values were normalized to the mean expression level of three housekeeping genes (*Gapdh*, *Rpl13A* and *Actb*).

50. Smyth, G.K. & Speed, T. Normalization of cDNA microarray data. *Methods* **31**, 265–273 (2003).